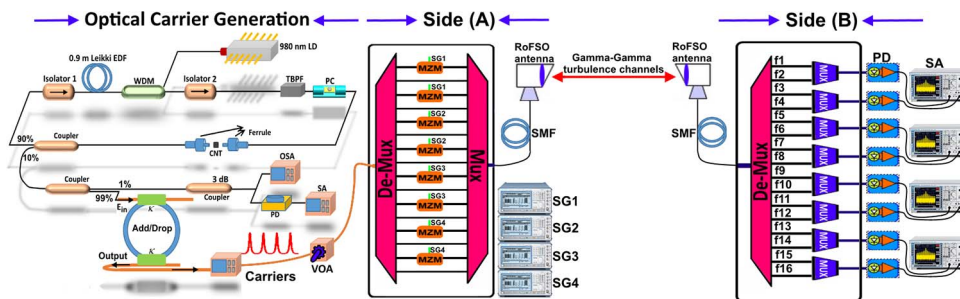


Carriers Generated by Mode-Locked Laser to Increase Serviceable Channels in Radio Over Free Space Optical Systems

Volume 7, Number 5, October 2015

H. Ahmad
M. R. K. Soltanian
I. S. Amiri
S. E. Alavi
A. R. Othman
A. S. M. Supa'at



DOI: 10.1109/JPHOT.2015.2484285
1943-0655 © 2015 IEEE

Carriers Generated by Mode-Locked Laser to Increase Serviceable Channels in Radio Over Free Space Optical Systems

H. Ahmad,¹ M. R. K. Soltanian,¹ I. S. Amiri,¹ S. E. Alavi,²
A. R. Othman,³ and A. S. M. Supa'at⁴

¹Photonics Research Centre, University of Malaya, 50603 Kuala Lumpur, Malaysia

²Faculty of Electrical Engineering, Universiti Teknologi Malaysia, 81310 Johor Bahru, Malaysia

³Faculty of Electronics and Computer Engineering Universiti Teknikal Malaysia,
76100 Melaka, Malaysia

⁴Lightwave Communication Research Group, Faculty of Electrical Engineering,
Universiti Teknologi Malaysia, 81310 Johor Bahru, Malaysia

DOI: 10.1109/JPHOT.2015.2484285

1943-0655 © 2015 IEEE. Translations and content mining are permitted for academic research only.

Personal use is also permitted, but republication/redistribution requires IEEE permission.

See http://www.ieee.org/publications_standards/publications/rights/index.html for more information.

Manuscript received September 4, 2015; accepted September 27, 2015. Date of publication October 1, 2015; date of current version October 13, 2015. This work was supported by the University of Malaya/MOHE under Grant UM.C/625/1/HIR/MOHE/SCI/01, Grant RU016-2014, and Grant LRGS(2015)/NGOD/UM/KPT. The work of S. E. Alavi was supported by the Universiti Teknologi Malaysia PAS under Grant Q.J130000.2609.10J97. Corresponding authors: I. S. Amiri and S. E. Alavi (e-mail: isafiz@yahoo.com; sayedehsan@utm.my).

Abstract: Mode-locked optical carriers with applicability for radio over free space optics (RoFSO) systems have been produced via a ring laser cavity incorporating an add/drop filter. This technique of generation allowed for servicing of a greater number of channels in a wavelength-division multiplexing RoFSO system, and the carriers were able to travel in a free space channel with very little dispersion. Sixteen carriers, having a free spectral range (FSR) of 12.5 GHz and full-width at half-maximum (FWHM) of 250 MHz, were created. Eight of these 16 generated carriers were then separately modulated with eight orthogonal frequency-division multiplex signals and subsequently optically multiplexed and transmitted to a free space optic (FSO) channel using an FSO antenna. At the receiver side, the received signal was demultiplexed, and the performance of the system was analyzed via calculating the error vector magnitude and constellation diagram of the entire system.

Index Terms: Mode-locked laser pulse, add/drop filter, fiber laser loop.

1. Introduction

Over the past few years, broadband access providers have faced sustained demands for higher data rates due to a great variety of new bandwidth-hungry services and an accumulating number of end users [1], [2]. Free space optical (FSO) systems constitute a promising means to meet the upcoming requirements of broadband access. FSO links can be conveniently used to transmit radio frequency (RF) signals, referred to as radio-over-free space optics (RoFSO), where the physical connection by means of optical fiber cables is impractical due to high costs or other considerations. RoFSO capacity is similar to that of radio over fiber (RoF) with the difference being an absence of fiber medium, and it combines the advantages of high transmission capacity provided by optical device technologies with the ease of deployment due to wireless links [3].

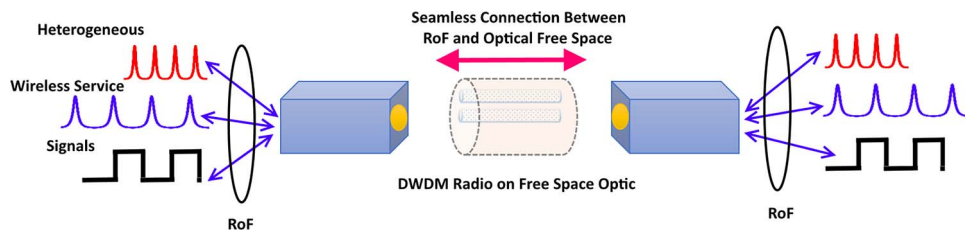


Fig. 1. Concept of radio over free space optics (RoFSO).

RoFSO also has applicability for indoor optical broadcasting, where a reported experimental demonstration involved a 15 meter pointed indoor optical wireless link in the 1550 nm wavelength region and comprised a uni-directional cable television (CATV) signal and a bi-directional link consisting of two 10 Gbps data links [4]. Performance of these emerging RoFSO systems for outdoor applications is highly influenced by the deployment environment characteristics, and has a particular susceptibility to weather conditions such as rain, snow, fog, dust particles, and so on, that deteriorate the link performance. In these situations, the transmitted optical beam may experience significant distortions due to the random refractive-index variations, commonly referred to as scintillation, which can lead to temporary deep fades in the received signal or even annihilation of the FSO link. Undoubtedly, one of the main challenges for RoFSO communication systems is overcoming the signal instability caused by atmospheric turbulence [5].

Preliminary experimental attempts for designing and evaluating an advanced dense wavelength-division multiplexing (DWDM) RoFSO system capable of simultaneously transmitting multiple RF signals carrying various broadband wireless services, including ISDB-T signals, cellular phone, wireless LAN, terrestrial digital broadcasting, and upcoming wireless services, over a 1 km FSO link were reported in [3] and [6]. Fig. 1 illustrates the concept of an advanced DWDM RoFSO link system detailed in [3].

RoFSO involves the direct optical amplification and emission of RoF signals into free space, and also the direct focusing of the received optical beams into the core of an SMF. A common technique for broadband access is orthogonal frequency division multiplexing (OFDM), which is robust against frequency selective fading and narrow-band interference, and has high channel efficiency [7]. It is used mainly in digital terrestrial TV broadcasting and complies with IEEE 802.11 local area network (LAN) and IEEE 802.16 standards.

Utilization of OFDM for RoFSO links was proposed and experimentally demonstrated in [8], [9]. One report [8] described the first in-field experiment of OFDM over FSO channels at a rate of 300 Mb/s over a range of 1.87 km. Another paper [9] reported on closed-form bit error probability (BEP) and outage probability expressions, modeled by the gamma-gamma distribution and taking into account optical noises, laser diode nonlinear distortion, and atmospheric turbulence effect on the FSO channel. Such results are useful for designing, predicting, and evaluating a RoFSO system's ability to transmit OFDM-based wireless services over turbulent FSO links under actual conditions.

While recent works have evolved the OFDM-based RoFSO technology in both indoor and outdoor applications, they have mostly focused on issues related to possible implementation rather than increasing the number of services in the whole RoFSO system. Since RoFSO is essentially analog transmission links, a major concern is achieving sufficiently stable and reliable signals. One possible solution to increase the number of wavelength division multiplexer (WDM) services is to generate more optical carriers in the transmitter section namely comb source generation. Multicarrier optical sources with narrow channel spacing have emerged to meet demands from networks with dense wavelength-division-multiplexing (WDM) and super dense WDM. Many solutions have been proposed to achieve low-cost compact multicarrier optical sources that would provide all the channels required by optical communication standards. These schemes are based on supercontinuum (SC) generation [10], nonlinear spectral broadening of intensity modulated signals [11], hybrid modulation with LiNbO₃ modulators [12], and phase

modulation in a regenerative erbium-doped fiber amplifier loop [13]. The proposed setup in this paper provides simple and efficient wide wavelength range due to generating mode-locked laser. Consequently, by launching generated mode-locked laser into pre-designed add/drop microring resonator filter with various diameters, the different phase-correlated optical carriers source with different spacing will be achieved.

Methods for producing mode-locking in a laser may be classified as either “active” or “passive” [14]. Active methods typically involve using an external signal to induce a modulation of the intracavity light. Passive methods do not use an external signal, but rely on placing some element as saturable absorber into the laser cavity which causes self-modulation of the light. Typically, pulsed fiber lasers are either mode-locked or Q-switched. Mode-locked outputs are desired in scenarios where ultra-fast pulses are desired, although this comes at the cost of the pulse power.

Fiber lasers have a number of qualities which make them attractive for ultrashort pulse generation via active or passive mode locking. They can be fabricated with low cost and can be very compact and rugged-particularly if free-space optics are not used. Considering the fiber laser cavity, each time the pulse hits the output coupler mirror, a usable pulse is emitted, so that a regular pulse train leaves the laser. For true soliton mode locking [15], these soliton shaping effects play a dominant role, and the pulse duration is nearly independent of other parameters. A saturable absorber is required for starting and stabilizing the mode locking. Each time the pulse hits the saturable absorber, it saturates the absorption, thus temporarily reducing the losses. Compared with active mode locking, the technique of passive mode locking allows the generation of much shorter pulses [16], essentially because of a saturable absorber. The necessary limitation of nonlinear phase shifts, combined with the fundamental soliton condition, implies certain scaling laws for soliton mode-locked lasers. For mode-locked fiber lasers, on the other hand, the nonlinear phase shifts are strong enough in the regime of multiple picoseconds and typically become too strong for pulse durations well below 1 ps. Erbium-doped fiber (EDF), exhibit a broad gain bandwidth, with a maximum either at 1535 nm or at some longer wavelength such as 1550 nm-depending on the composition of the fiber core and on the inversion level, which itself is determined by fiber length, doping concentration and resonator losses. Since the stability of mode-locked laser investigated by [17], [18], the main objective of this work is to generate a tuneable number of multi-carriers, as well as increased stability for these carriers. Consequently, the increase in serviceable WDM channels can provide a dramatic upsurge to the capability of entire RoFSO systems. The benefits of using a comb source in our design instead of a WDM source for WDM-FSO transmission is the inherent reduction of laser transmitters in the optical line terminal of common WDM systems and also the reduced cost of wavelength stabilization.

In this work, the generation of many optical carriers to be applied in RoFSO system necessitated the use of a ring laser EDF cavity incorporated with an optical add/drop filter. The generation of carriers from the mode-locked laser is performed experimentally, while the optical add/drop filter, modulation and transmission of the signals via the RoFSO have investigated and modeled theoretically. Several reports [19]–[21] recommended exploiting optical carriers in order to create a spectrum of light over a wide range with a very high stability, and this suggestion was duly realized in this work. Moreover, control of the ring laser was achieved by manipulating variable parameters of the system [22]. This paper details a performance evaluation analysis of the RoFSO system when simultaneous transmitting multiple OFDM signals were modulating the optical carriers. Additionally, the system design specifications and operating environment were taken into account for the derivation of the presented error vector magnitude (EVM) for various FSO links.

2. Optical Multicarrier Generation Principals

The description of mode-locking, in terms of a pulse spectrum that evolves with time, can be transformed into a description of a pulse with a temporal envelope that evolves on a time scale

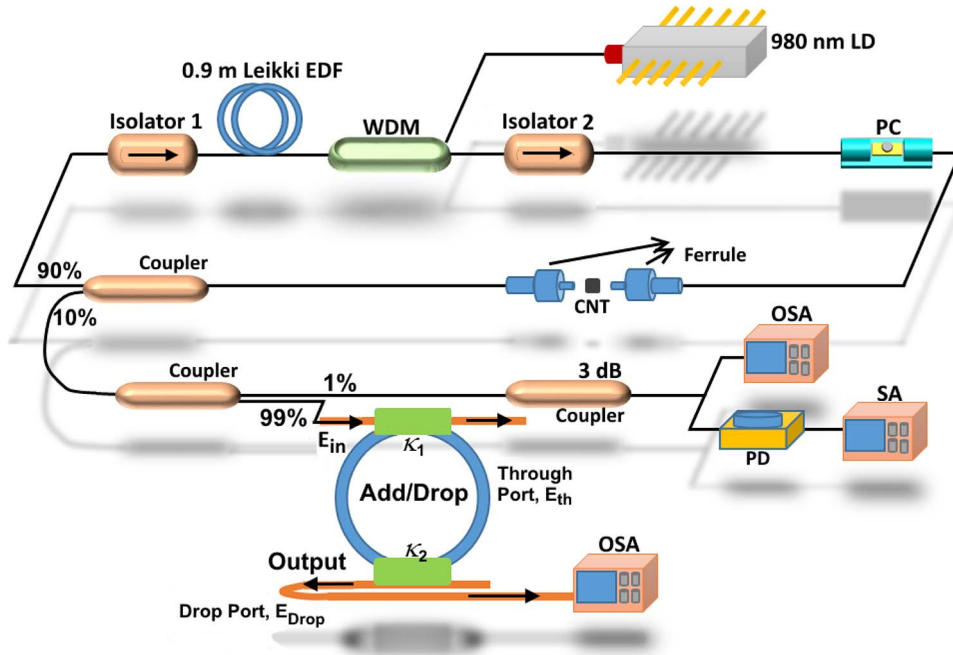


Fig. 2. System setup for multi-carrier generation.

much longer than the pulse width. This conversion is accomplished by means of a Fourier-transform, in which the Fourier-transform pairs possess the mathematical forms [23], [24]

$$\alpha(t) = \int \exp(j\Omega t) A(\Omega) d\Omega \quad (1)$$

$$A(\Omega) = \frac{1}{2\pi} \int \exp(-j\Omega t) \alpha(t) dt. \quad (2)$$

If ΔA is used to denote the combined changes of the amplitude per round-trip, then

$$\Delta A = T_R \frac{\partial}{\partial T} A(T, t)$$

with the Haus master equation describing pulse evolution for mode-locking as

$$T_R \frac{\partial}{\partial T} A(T, t) = \left(-jD \frac{\partial^2}{\partial t^2} + j\delta |A|^2 \right) A + \left(g - l + \frac{g}{\Omega_g^2} \frac{\partial^2}{\partial t^2} - q(T, t) \right) A \quad (3)$$

where $A(T, t)$ is a slowly varying electric field envelope denoted as E_{in} in (5) described later in this paper, T is a long-term time variable (used for a slowly varying envelope approximation), t is a short-term time variable, D is the group delay dispersion (GDD), δ is the self-phase modulation (SPM) coefficient, g is the small-signal electric field gain coefficient (as in gain = 1 + g), l is the constant small signal cavity loss, $q(T, t)$ is the saturable loss, T_R is the cavity round-trip time, and Ω_g is the full width at half maximum (FWHM) bandwidth of the gain medium [25].

2.1. Experimental Setup To Generate Multi Optical Carriers

Fig. 2 shows the setup employed for multi-carrier generation, in which the fiber laser layout resulted in a mode-locked laser connected to a single add/drop filter. The laser utilized an active gain medium consisting of a 0.9 m long highly doped Leikki Er80-8/125 EDF that possessed an

NA of 0.21 to 0.24, mode field diameter of 5.7–6.6 μm at 1550 nm, and an absorption coefficient of 84 dB/m at 980 nm. The EDF was pumped backward by a Lumics 980 nm laser diode (LD) through a WDM. One end of the EDF was connected to the common output of the WDM, while the other end was connected to an isolator to ensure no signals propagated in the opposite direction through the EDF. The isolator connected to the WDM was used to avoid any unwanted back reflection toward the gain medium. This isolator was in turn connected to a polarization controller (PC), which was subsequently linked to a carbon nanotube (CNT) embedded between two ferrules. The output of the embedded CNT was guided toward a 90:10 coupler, which extracted a portion of the signal for analysis. The 90% port was connected to an isolator, which was then connected to the gain medium. This loop completed the laser cavity.

In order to generate the multi-carriers, the 10% port was divided into two portions using a 99:1 coupler, and thereafter the resulting 99% port was forwarded to the add/drop filter for generation of evenly spaced multi-carriers with 12.5 GHz spacing while the 1% part was utilized for monitoring purposes. In order to monitor the extracted output prior to the add/drop stage, the generated mode-locked signal was divided into two evenly powered portions using a 3 dB coupler; one portion was directed to an optical spectrum analyzer (OSA) (model YOKOGAWA AQ6370B) while the other segment travelled to a photodiode (HP Lightwave Detector DC-6 GHz) and finally a radio frequency-spectrum analyzer (RF-SA Anritsu MS2683A). This separation process allowed for calculation of the average output power, the spectrum in the time domain and radio frequency spectrum via analysis. An OSA (model YOKOGAWA AQ6370B) was used to monitor the generated multi-carriers following the add/drop step.

2.2. Add/Drop Filter Characterization

There have been several techniques reported up to now for the generation of multi-carriers used in optical communications [26]–[30]. One method to generate optical multi-carriers lies in adjusting parameters of Mach–Zehnder modulators (MZM) such as biasing point [31]–[33]. Microring resonators (MRRs) have attracted considerable attention in the field of optical communications [34], [35]. In addition to the superior stability and beam quality associated with multi-carriers generated by MRRs, a chief objective of using MRR systems lies in producing greater numbers of multi-carriers than have been previously reported. Achieving such an objective will lead to an increase in capability of entire integrated systems [36]–[39]. A single microring resonator configuration as add/drop filter connected to the fiber laser loop was constructed by the InGaAsP/InP waveguide using optical couplers. The ring resonator circumference is labeled as L , while the input mode-locked pulse into the ring resonator is given by $E_{in}(t)$, and the output signal is expressed by $E_{out}(t)$ [40]. The total refractive index (n) of the add/drop filter is given by

$$n = n_0 + n_2 I = n_0 + \left(\frac{n_2}{A_{\text{eff}}} \right) P \quad (4)$$

where n_0 and n_2 are the linear and nonlinear refractive indices respectively, I and P are the optical intensity and optical power, respectively, and A_{eff} represents the effective mode core area of the device. In the case of add/drop events, the effective mode core area given by A_{eff} ranges from 0.10 to 0.25 μm^2 in terms of practical material parameters (InGaAsP/InP) [41]. When a laser pulse is injected and propagates within an add/drop component, the resonant output is formed for each round-trip. The normalized output of the light field is defined as the ratio between the output and input fields ($E_{out}(t)$ and $E_{in}(t)$) in each round-trip. Thus, this normalized output can be expressed as

$$\frac{E_{out}(t)}{E_{in}(t)} = \sqrt{(1 - \gamma) \times \left[1 - \frac{(1 - (1 - \gamma)x^2)\kappa}{(1 - x\sqrt{1 - \gamma}\sqrt{1 - \kappa})^2 + 4x\sqrt{1 - \gamma}\sqrt{1 - \kappa}\sin^2\left(\frac{\phi}{2}\right)} \right]}. \quad (5)$$

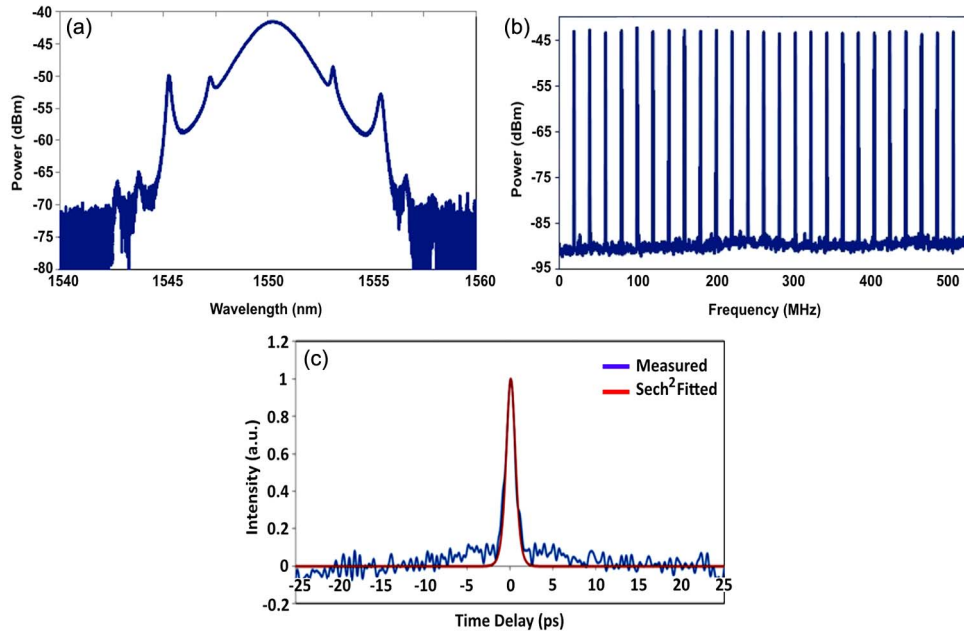


Fig. 3. (a) Spectrum of experimentally generated mode-locked laser pulse. (b) RF signals generated from the mode-locked laser pulses. (c) Autocorrelation trace for the generated mode-locked laser.

Here, κ is the coupling coefficient, $x = \exp(-\alpha L/2)^2$ represents a round-trip loss coefficient, $\phi = \phi_0 + \phi_{NL}$, where $\phi_0 = kLn_0$ and $\phi_{NL} = kLn_2|E_{in}|^2$ are the linear and nonlinear phase shifts respectively, and $k = 2\pi/\lambda$ is the wave number [42]. Introduction of an add/drop filter with appropriate parameters is proposed in order to retrieve signals from chaotic noise. The mode-locked laser output, which is shown in Fig. 3 as the OSA port, is inserted into the input port of the add/drop filter, and E_{th} and E_{drop} represent the resulting output electric fields of the system. The normalized power of the through and drop ports are then obtained as follows [43], [44]:

$$\left| \frac{E_{th}}{E_{in}} \right|^2 = \frac{1 - \kappa_1 - 2\sqrt{1 - \kappa_1}\sqrt{1 - \kappa_2}e^{-\frac{\alpha}{2}L_{ad}}\cos(k_n L_{ad}) + (1 - \kappa_2)e^{-\alpha L_{ad}}}{1 + (1 - \kappa_1)(1 - \kappa_2)e^{-\alpha L_{ad}} - 2\sqrt{1 - \kappa_1}\sqrt{1 - \kappa_2}e^{-\frac{\alpha}{2}L_{ad}}\cos(k_n L_{ad})} \quad (6)$$

$$\left| \frac{E_{th}}{E_{in}} \right|^2 = \frac{\kappa_1 \cdot \kappa_2 e^{-\frac{\alpha}{2}L_{ad}}}{1 + (1 - \kappa_1)(1 - \kappa_2)e^{-\alpha L_{ad}} - 2\sqrt{1 - \kappa_1}\sqrt{1 - \kappa_2}e^{-\frac{\alpha}{2}L_{ad}}\cos(k_n L_{ad})}. \quad (7)$$

Here, L_{ad} is the add/drop filter length, where $L_{ad} = 2\pi R_{ad}$ and κ_1 and κ_2 are the coupling coefficients. The waveguide (ring resonator) loss was $\alpha = 0.5 \text{ dBmm}^{-1}$, and the fractional coupler intensity loss was $\gamma = 0.1$ [45]–[47].

2.3. Experimental Results of Multi-Carriers Generation

The experimental spectrum of the mode-locked laser pulses is presented in Fig. 3(a). The generated mode-locked laser has asymmetric sidebands. Sideband asymmetry in a passively mode-locked soliton fiber ring laser has been carefully investigated in [48]. The power asymmetry in the sidebands can be explained based on a linear cavity transmission analysis. In the case of a laser cavity with a multi-birefringent beat length, the nonlinearity of the fiber introduces a nonlinear phase change [49], [50]. These observed mode-locked pulses were achieved at a threshold pump power of about 40 mW, with the optical spectrum having a very wide-band output together with multiple sidebands present, as can be seen in the figure. After

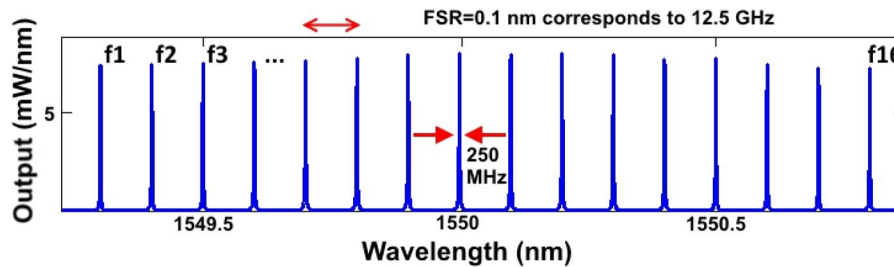


Fig. 4. Spectrum of the add/drop filter output signals using the input mode-locked laser.

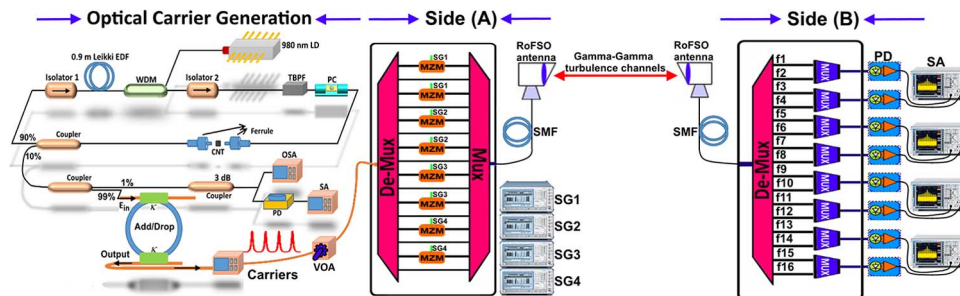


Fig. 5. RoFSO system setup.

photodetection, the frequency-spectrum analyzer was used to analyze the beating frequency for each of the two modes available in the mode-locked spectrum across a 0–500 MHz range, and the output is shown in Fig. 3(b). Here, the pulses have a free spectral range (FSR) of 20 MHz and FWHM of 350 KHz. Fig. 3(c) shows the autocorrelation trace of the generated mode-locked laser. The estimated pulse durations at the full-width at half maximum (FWHM) point is 810 fs. The autocorrelation trace and spectrum are well fitted by a pulse profile, indicating that mode-locked laser is generated.

Fig. 4 shows the results from the add/drop section, which possesses a coupling factor of $\kappa_1 = \kappa_2 = 0.1$, linear and nonlinear refractive indices of 3.34 and 2.2×10^{-17} respectively and radius of 1.2 mm, where such signals occur after the mode-locked laser pulse is input into the add/drop filter. The effective mode core area has been selected as $25 \mu\text{m}^2$. As can be seen from this figure, the bandwidth and FSR of the mode-locked pulses are enlarged. The finesse and Q-factor have been subsequently calculated in order to evaluate these signals.

The finesse (F), given by the ratio FSR over FWHM (FSR/FWHM), is approximately 50, and the Q-factor, which is the ratio of the resonant wavelength to the 3-dB bandwidth (FWHM), is about 7.73×10^5 . Such results are evidence of this newly proposed and demonstrated system having high performance. Therefore, the add/drop filter can be used to enlarge the FSR by splitting the input spectrum mode-locked laser. When the wavelength of an incident optical signal propagating within the waveguide overlaps a resonant wavelength mode of the ring, the signal can be partially or entirely removed from the waveguide. This functionality is particularly well suited for filtering and switching wavelength division multiplexing (WDM) optical signals and also multiple-wavelength optical packets. In the work described in this paper, 16 carriers with the frequency spacing of 12.5 GHz ($f_n = f_{n-1} + 12.5 \text{ GHz}$) were generated in the optical domain, where f_1 was located at 193.326 THz, and f_{16} was located at 193.414 THz.

3. RoFSO System Setup

The system setup for the RoFSO when simultaneously transmitting multiple eight OFDM signals is shown in Fig. 5. This system involved a 1.2 km line-of-sight (LOS) outdoor FSO wireless link

TABLE 1

OFDM signal parameters

| Parameters | Value |
|---------------------------------------|-------------|
| DAC sampling rate | 10-GSa/s |
| IFFT size | 256 |
| sub-carrier frequency separation | 39.0625-MHz |
| Number of generated subcarriers at BB | 64 |
| Bandwidth | 2.5-GHz |

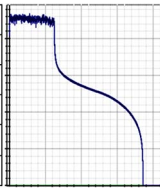
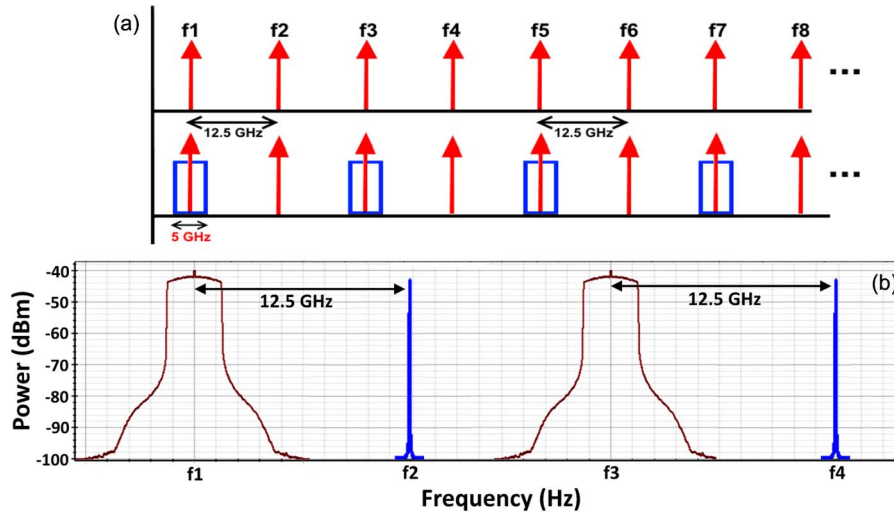



Fig. 6. (a) Optical carriers separation and modulation. (b) Modulated OFDM signals.

that could be considered as gamma-gamma turbulence channels. In this case, the probability density function (pdf) of turbulence channel h_a is given as [51]

$$f_{h_a}(h_a) = \frac{2\alpha\beta^{(\alpha+\beta)/2}}{\Gamma(\alpha)\Gamma(\beta)} (h_a)^{(\alpha+\beta)/2-1} K_{\alpha-\beta}(2\sqrt{\alpha\beta h_a})$$

where $K_{\alpha-\beta}(\cdot)$ is the modified Bessel function of the second kind, and $1/\beta$ and $1/\alpha$ are the variances of the small and large scale eddies, respectively. It was shown by [52] that the Gamma-Gamma pdf is in close agreement with measurements under a variety of turbulence conditions. Tektronix AWG7102 arbitrary waveform generator (AWG) for producing the base band (BB) OFDM with 16 quadrature amplitude modulation (QAM) mapping for wireless service signals under investigation were placed in one side (Side A in the figure). The parameters for OFDM signals are listed in Table 1.

According to Table 1 and by considering QAM signaling for OFDM transmission in case of one channel, the data rate can be exceeded up to 2.5 Gbit/sec. Therefore, for 16 DWDM channels the total capacity is about 16×2.5 Gbit/sec = 40 Gbit/sec.

Since the baseband OFDM signal was complex and bipolar while a real and positive RF signal is required to modulate the optical carriers in an optical link, generating the real OFDM signal necessitated a Hermitian symmetry operation and transformation of the OFDM signal to unipolar. As such, a DC bias was added to the OFDM signal (DC-OFDM) so that the resulting signal becomes positive.

In side A, 16 generated carriers were separated using a demultiplexer, and, as shown in Fig. 6, eight of them ($f_1, f_3, f_5, f_7, f_9, f_{11}, f_{13}, f_{15}$) were intensity modulated via their corresponding OFDM signal.

TABLE 2

Specification of RoFSO antenna

| Parameter | Specification |
|----------------------|--------------------------|
| Operating wavelength | 1550 nm |
| Transmission power | 100 mW (20 dBm) |
| Antenna aperture | 80 mm |
| Coupling losses | 5 dB |
| Beam divergence | $\pm 47.3 \mu\text{rad}$ |

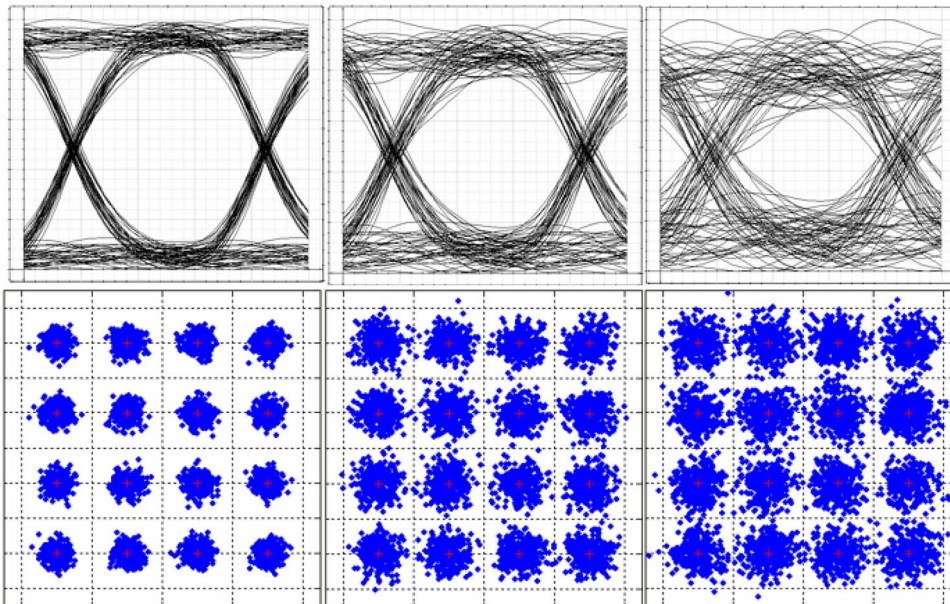
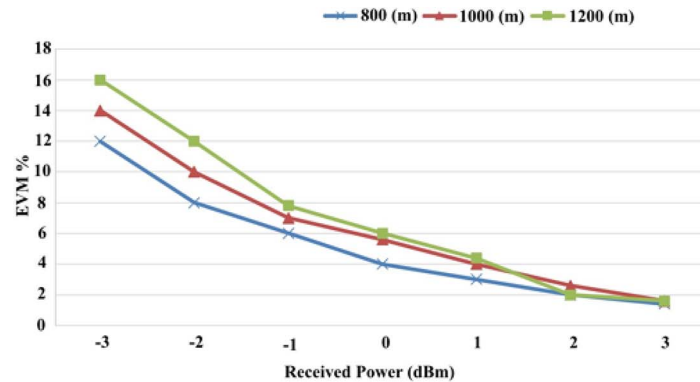


Fig. 7. Measured EVM for three different FSO lengths with associated eye diagrams.

After selected carriers were modulated, these modulated carriers along with unmodulated one were multiplexed and transmitted to the RoFSO antenna using single-mode fibers (SMFs). At both ends of RoFSO antennas, collimators possessing the parameters for the RoFSO channel shown in Table 2 were used to couple the optical wireless signal into SMF. These RoFSO antennas consisted of boost and post amplifiers and an optical circulator to separate transmit and receive signals.

Signal analyzers and other measurement devices and equipment were situated in the other side (side B in Fig. 5), where the received optical signal was demultiplexed via collector/splitter

nodes. Subsequently, every two carriers (one modulated and one unmodulated) with a 12.5 GHz frequency difference (like f_1 and f_2) were multiplexed and converted to an RF signal using a photodiode (PD). The RF signal, which was located at 12.5 GHz, was acquired by beating the two optical beams by a 12.5 GHz frequency distance. As a result, eight RoFSO channels were acquired for further processing in the receiver part.

The system error vector magnitude (EVM) performance for the downlink stream of the OFDM-based RoFSO system for one signal was tested. The test was based on the variation of the FSO length in three distances, these being 800, 1000, and 1200 m, and the EVM variation result relationship with received power is shown in Fig. 7.

As shown in Fig. 7, the acceptable EVM of less than 10% for three different FSO lengths was achieved for at least (-1) dBm received power, and the differences in timing and amplitude from bit to bit cause the eye opening to shrink. For the Fig 7, there is an open eye for each case that shows a possible successful reception.

4. Conclusion

A laser cavity incorporating an add/drop filter was manipulated in order to generate suitable mode-locked optical carriers for a RoFSO system. The produced carriers possessed sufficient stability with low dispersion for traveling in a free space channel. Furthermore, the production technique provided for greater number of channels for servicing in a WDM RoFSO system. For this purpose, sixteen mode-locked carriers with an FSR of 12.5 GHz and FWHM of 250 MHz were generated. Eight of these sixteen carriers were separately modulated with eight OFDM signals, and then were optically multiplexed and transmitted to an FSO channel using an FSO antenna. It was observed that the received RF signal performance had acceptable EVM results, and therefore, this proposed method of production and communication can be used to service extra channels in RoFSO systems.

References

- [1] N. Madamopoulos *et al.*, "Applications of large-scale optical 3D-MEMS switches in fiber-based broadband-access networks," *Photon. Netw. Commun.*, vol. 19, no. 1, pp. 62–73, Feb. 2010.
- [2] E. Wong, "Next-generation broadband access networks and technologies," *J. Lightwave Technol.*, vol. 30, no. 4, pp. 597–608, Feb. 2012.
- [3] K. Kazaura *et al.*, "RoFSO: A universal platform for convergence of fiber and free-space optical communication networks," *IEEE Commun. Mag.*, vol. 48, no. 2, pp. 130–137, Feb. 2010.
- [4] M. S. Chowdhury, M. Kavehrad, W. Zhang, and P. Deng, "Combined CATV and very-high-speed data transmission over a 1550-nm wavelength indoor optical wireless link," in *Proc. SPIE OPTO*, 2014, Art ID. 901009.
- [5] C. B. Naila, K. Wakamori, M. Matsumoto, A. Bekkali, and K. Tsukamoto, "Transmission analysis of digital TV signals over a radio-on-FSO channel," *IEEE Commun. Mag.*, vol. 50, no. 8, pp. 137–144, Aug. 2012.
- [6] M. Matsumoto *et al.*, "Experimental investigation on a radio-on-free-space optical system suitable for provision of ubiquitous wireless services," *PIERS Online*, vol. 6, no. 5, pp. 400–405, 2010.
- [7] S. E. Alavi *et al.*, "W-band OFDM for radio-over-fibre direct-detection link enabled by frequency nonupling optical up-conversion," *IEEE Photon. J.*, vol. 6, no. 6, Dec. 2014, Art ID. 7903908.
- [8] A. Mostafa and S. Hranilovic, "In-field demonstration of OFDM-over-FSO," *IEEE Photon. Technol. Lett.*, vol. 24, no. 8, pp. 709–711, Apr. 2012.
- [9] A. Bekkali, C. Ben Naila, K. Kazaura, K. Wakamori, and M. Matsumoto, "Transmission analysis of OFDM-based wireless services over turbulent radio-on-FSO links modeled by Gamma-Gamma distribution," *IEEE Photonics J.*, vol. 2, no. 3, pp. 510–520, Jun. 2010.
- [10] K. Mori, H. Takara, and S. Kawanishi, "Analysis and design of supercontinuum pulse generation in a single-mode optical fiber," *J. Opt. Soc. Amer. B*, vol. 18, no. 12, pp. 1780–1792, 2001.
- [11] J. Veselka and S. Korotky, "A multiwavelength source having precise channel spacing for WDM systems," *IEEE Photon. Technol. Lett.*, vol. 10, no. 7, pp. 958–960, Jul. 1998.
- [12] M. Fujiwara *et al.*, "Optical carrier supply module using flattened optical multicarrier generation based on sinusoidal amplitude and phase hybrid modulation," *J. Lightwave Technol.*, vol. 21, no. 11, pp. 2705–2714, Nov. 2003.
- [13] S. Bennett *et al.*, "1.8-THz bandwidth, zero-frequency error, tunable optical comb generator for DWDM applications," *IEEE Photon. Technol. Lett.*, vol. 11, no. 5, pp. 551–553, May 1999.
- [14] W. E. Lamb, "Theory of an optical maser," *Phys. Rev.*, vol. 134, no. 6A, pp. A1429–A1450, Jun. 1964.
- [15] F. Kärtner, I. Jung, and U. Keller, "Soliton mode-locking with saturable absorbers," *IEEE J. Sel. Topics Quantum Electron.*, vol. 2, no. 3, pp. 540–556, Sep. 1996.

- [16] S. Arahira, Y. Matsui, and Y. Ogawa, "Mode-locking at very high repetition rates more than terahertz in passively mode-locked distributed-Bragg-reflector laser diodes," *IEEE J. Quantum Electron.*, vol. 32, no. 7, pp. 1211–1224, Jul. 1996.
- [17] J. Hou *et al.*, "High-stability passively mode-locked laser based on dual SESAM," *Appl. Phys. B*, vol. 116, no. 2, pp. 347–351, Aug. 2014.
- [18] P. Datta, S. Mukhopadhyay, and A. Agnesi, "Stability regime study of a nonlinear mirror mode-locked laser," *Opt. Commun.*, vol. 230, no. 4–6, pp. 411–418, Feb. 2004.
- [19] L. Kong, X. Xiao, and C. Yang, "Operating regime analysis of a mode-locking fiber laser using a difference equation model," *J. Opt.*, vol. 13, no. 10, 2011, Art. ID. 105201.
- [20] M. Soltanian, I. S. Amiri, S. E. Alavi, and H. Ahmad, "All optical ultra-wideband signal generation and transmission using mode-locked laser incorporated with add-drop Microring Resonator (MRR)," *Laser Phys. Lett.*, vol. 12, no. 6, 2015, Art. ID. 065105.
- [21] S. E. Alavi, I. S. Amiri, S. M. Idrus, and A. S. M. Supa'at, "Generation and wired/wireless transmission of IEEE 802.16m signal using solitons generated by microring resonator," *Opt. Quantum Electron.*, vol. 47, no. 5, pp. 975–984, May 2014.
- [22] A. Syed, G. Chaitanya, and M. Sayeh, "All optical digital logic gates library," *J. Opt.*, vol. 41, no. 3, pp. 142–147, Sep. 2012.
- [23] H. A. Haus, "Mode-locking of lasers," *IEEE J. Sel. Topics Quantum Electron.*, vol. 6, no. 6, pp. 1173–1185, Nov./Dec. 2000.
- [24] M. Iqbal, Z. Zheng, and T. Yu, "Modeling of mode-locked lasers," in *Proc. 7th WSEAS Int. Conf. Simul., Modell. Optim.*, 2007, pp. 474–479.
- [25] I. S. Amiri, M. R. K. Soltanian, S. E. Alavi, and H. Ahmad, "Multi wavelength mode-lock soliton generation using fiber laser loop coupled to an add-drop ring resonator," *Opt. Quantum Electron.*, vol. 47, no. 8, pp. 2455–2464, Aug. 2015.
- [26] Z. Cao *et al.*, "WDM-RoF-PON architecture for flexible wireless and wire-line layout," *J. Opt. Commun. Netw.*, vol. 2, no. 2, pp. 117–121, Feb. 2010.
- [27] J. Yu *et al.*, "Demonstration of a novel WDM passive optical network architecture with source-free optical network units," *IEEE Photon. Technol. Lett.*, vol. 19, no. 8, pp. 571–573, Apr. 2007.
- [28] M. Zhu *et al.*, "Efficient delivery of integrated wired and wireless services in UDWDM-RoF-PON coherent access network," *IEEE Photon. Technol. Lett.*, vol. 24, no. 13, pp. 1127–1129, Jul. 2012.
- [29] W. Ji and J. Chang, "The radio-on-fiber-wavelength-division-multiplexed-passive-optical network (WDM-RoF-PON) for wireless and wire layout with linearly-polarized dual-wavelength fiber laser and carrier reusing," *Opt. Laser Technol.*, vol. 49, pp. 301–306, Jul. 2013.
- [30] Y. Xiao and J. Yu, "A novel WDM-ROF-PON architecture based on 16QAM-OFDM modulation for bidirectional access networks," *Opt. Commun.*, vol. 295, pp. 99–103, May 2013.
- [31] J. H. Zhu, X. G. Huang, and J. L. Xie, "A full-duplex radio-over-fiber system based on dual quadrupling-frequency," *Opt. Commun.*, vol. 284, no. 3, pp. 729–734, Feb. 2011.
- [32] W. J. Fang and X. G. Huang, "Transmission of multibands wired and wireless orthogonal frequency division multiplexing signals using a full-duplex dense wavelength division multiplexing radio-over-fiber system," *Opt. Eng.*, vol. 52, no. 1, 2013, Art. ID. 015003.
- [33] L. Zhang, X. Hu, P. Cao, Q. Chang, and Y. Su, "Simultaneous generation of independent wired and 60-GHz wireless signals in an integrated WDM-PON-RoF system based on frequency-sextupling and OCS-DPSK modulation," *Opt. Exp.*, vol. 20, no. 13, pp. 14648–14655, Jun. 2012.
- [34] R. Ji *et al.*, "Microring-resonator-based four-port optical router for photonic networks-on-chip," *Opt. Exp.*, vol. 19, no. 20, pp. 18945–18955, Sep. 2011.
- [35] X. Cai *et al.*, "Integrated compact optical vortex beam emitters," *Science*, vol. 338, no. 6105, pp. 363–366, Oct. 2012.
- [36] F. Ferdous *et al.*, "Spectral line-by-line pulse shaping of on-chip microresonator frequency combs," *Nature Photon.*, vol. 5, pp. 770–776, 2011.
- [37] T. J. Kippenberg, R. Holzwarth, and S. Diddams, "Microresonator-based optical frequency combs," *Science*, vol. 332, no. 6029, pp. 555–559, Apr. 2011.
- [38] J. S. Levy *et al.*, "CMOS-compatible multiple-wavelength oscillator for on-chip optical interconnects," *Nature Photon.*, vol. 4, pp. 37–40, 2010.
- [39] B. G. Lee, A. Biberman, P. Dong, M. Lipson, and K. Bergman, "All-optical comb switch for multiwavelength message routing in silicon photonic networks," *IEEE Photon. Technol. Lett.*, vol. 20, no. 10, pp. 767–769, May 2008.
- [40] I. S. Amiri and A. Afrozeh, *Ring Resonator Systems to Perform the Optical Communication Enhancement Using Soliton*. Singapore: Springer-Verlag, 2015.
- [41] I. S. Amiri, S. E. Alavi, N. Faisal, A. S. M. Supa'at, and H. Ahmad, "All-optical generation of two IEEE802.11n signals for 2×2 MIMO-RoF via MRR system," *IEEE Photon. J.*, vol. 6, no. 6, Dec. 2014, Art. ID. 7903611.
- [42] I. S. Amiri *et al.*, "W-band OFDM transmission for radio-over-fiber link using solitonic millimeter wave generated by MRR," *IEEE J. Quantum Electron.*, vol. 50, no. 8, pp. 622–628, Aug. 2014.
- [43] S. E. Alavi, I. S. Amiri, H. Ahmad, A. S. M. Supa'at, and N. Faisal, "Generation and transmission of 3×3 W-band MIMO-OFDM-RoF signals using micro-ring resonators," *Appl. Opt.*, vol. 53, no. 34, pp. 8049–8054, 2014.
- [44] I. S. Amiri *et al.*, "Increment of access points in integrated system of wavelength division multiplexed passive optical network radio over fiber," *Sci. Rep.*, vol. 5, Jul. 2015, Art. ID. 11897.
- [45] K. Ogusu and Y. Oda, "Modeling of the dynamic transmission properties of chalcogenide ring resonators in the presence of fast and slow nonlinearities," *Opt. Exp.*, vol. 19, no. 2, pp. 649–659, Jan. 2011.
- [46] I. S. Amiri, S. E. Alavi, S. M. Idrus, A. Nikoukar, and J. Ali, "IEEE 802.15.3c WPAN standard using millimeter optical pulsed signal generated by a panda ring resonator," *IEEE Photonics J.*, vol. 5, no. 5, Oct. 2013, Art. ID. 7901912.
- [47] P. Yupapin, C. Teeka, and J. Ali, *Nanoscale Nonlinear Panda Ring Resonator*. Boca Raton, FL, USA: CRC, 2012.
- [48] W. Man, H. Tam, M. Demokan, P. Wai, and D. Tang, "Mechanism of intrinsic wavelength tuning and sideband asymmetry in a passively mode-locked soliton fiber ring laser," *J. Opt. Soc. Amer. B*, vol. 17, no. 1, pp. 28–33, 2000.

- [49] M. Hofer, M. E. Fermann, F. Haberl, M. Ober, and A. Schmidt, "Mode locking with cross-phase and self-phase modulation," *Opt. Lett.*, vol. 16, no. 7, pp. 502–504, 1991.
- [50] R. Stolen, J. Botineau, and A. Ashkin, "Intensity discrimination of optical pulses with birefringent fibers," *Opt. Lett.*, vol. 7, no. 10, pp. 512–514, 1982.
- [51] A. Farid and S. Hranilovic, "Outage capacity optimization for free-space optical links with pointing errors," *J. Lightwave Technol.*, vol. 25, no. 7, pp. 1702–1710, Jul. 2007.
- [52] M. Al-Habash, L. C. Andrews, and R. L. Phillips, "Mathematical model for the irradiance probability density function of a laser beam propagating through turbulent media," *Opt. Eng.*, vol. 40, no. 8, pp. 1554–1562, 2001.